Earth Pressures and Design Considerations
of Narrow MSE Walls

Ken T. Kniss [1], Kuo-Hsin Yang [2], Stephen G. Wright[3] and Jorge G. Zornberg[4]

ABSTRACT

The design methodology for earth retaining structures placed in front of a stable slope or wall with limited space is unclear at present. A study, sponsored by TxDOT, has been conducted to investigate the earth pressure against walls in narrow spaces using the finite element method. The first part of this paper presents a comparison of earth pressure predictions by the finite element method with experimental data and theory based on soil arching. In the second part of the paper, the effect of aspect ratio on earth pressures for at-rest conditions are investigated. Earth pressure theories that do not consider "arching effects" may be overly conservative when applied to narrow walls. Calculated earth pressures from this study are compared to the design earth pressures according to FHWA MSE wall design guidelines.

Keywords: narrow retaining wall, lateral earth pressure, arching effect

1. Master Student, Civil Dept., The University of Texas at Austin, kkniss@mail.utexas.edu
2. Ph.D. Candidate, Civil Dept., The University of Texas at Austin, khyang@mail.utexas.edu
3. Professor, Civil Dept., The University of Texas at Austin, swright@mail.utexas.edu
4. Associate Professor, Civil Dept., The University of Texas at Austin, zornberg@mail.utexas.edu

INTRODUCTION

As the population increases and development of urban areas becomes a priority, transportation demand has increased which has led to widening of existing highways to improve traffic flow. One solution is to build mechanically stabilized earth (MSE) walls in front of previously stabilized walls. The acceptance of MSE walls has been driven by a number of factors, including aesthetics, reliability, cost, construction techniques, seismic performance, and the ability to tolerate large deformations without structural distress. However, due to the high cost of addition right-of-way and limited space available at the job site, construction of earth retaining walls is done within a constrained space. An example of narrow retaining walls is illustrated in Figure 1.

Research is being conducted at the University of Texas at Austin, sponsored by TxDOT, to investigate the design of narrow retaining walls in front of stable faces. The motivation for the research is twofold. First, the construction of narrow retaining walls is not addressed in the FHWA guidelines (Elias et al., 2001). The existing state-of-practice suggests a minimum wall width and MSE reinforcement length equal to 70 percent of the wall height. Second, the design methodology to construct narrow earth retaining structures in front of a stable wall is unclear. Various studies suggest the mechanics of narrow retaining walls is different from traditional walls, and earth pressures are different from conventional earth pressures due to the wall geometry.
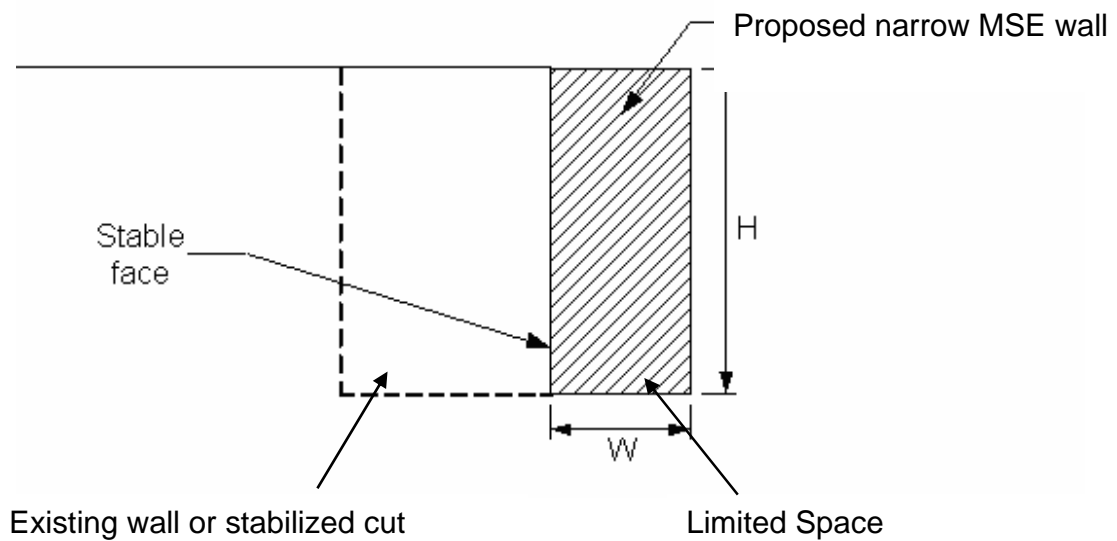
Figure 1 - Illustration of proposed narrow MSE wall in front of a stabilized face

BACKGROUND

The study of pressure in a constrained space originated from the agricultural study of silos, but geotechnical engineers also recognized its importance. Some recent studies on this topic are discussed in the following pages. Frydman and Keissar (1987) conducted a series of centrifuge tests to investigate the earth pressure on retaining walls near rock faces in both the at-rest and active condition. The aspect ratio of the soil behind the wall (L/H) was varied among tests from 0.1 to 1.1. Frydman and Keissar found that the measured earth pressure decreased with depth from theoretical at-rest values near the top of the wall. This phenomenon was attributed to an arching effect

Take and Valsangkar (2001) also performed a series of centrifuge tests to study the earth pressure on unyielding retaining walls with narrow backfills. The wall aspects ratios ranged from 0.10 to 0.70. Their tests agreed with Frydman's finding that the measured earth pressure decreased from the theoretical at-rest value with increasing depth below

the surface. In addition, measurements of lateral earth pressure acting on the unyielding model retaining walls showed good agreement with the arching theory by Janssen described in the next section.

Woodruff (2003) performed a comprehensive series of centrifuge model tests on reinforced soil walls adjacent to a stable face ("shoring"). Woodruff tested 24 different walls with reinforcement lengths (wall widths) ranging from 0.17 to 0.90 times the wall height. Tests were performed with reinforcement of three different tensile strengths, and reinforcement layouts involving five different vertical spacings. He observed that when the wall aspect ratio decreased below 0.26, the failure mode transformed from internal failure to external failure. The transformation may be the result of decreasing lateral earth pressures, but Woodruff was not able to comment on the earth pressures because he did not measure them.

Leshchinsky and Hu (2003) performed a series of limit equilibrium analyses of MSE walls with limited space between the retaining wall and a stable face. Based on their limit equilibrium analyses Leshchinsky and Hu presented a series of design charts for the earth pressure coefficient expressed as a ratio of the lateral earth pressure coefficient to the conventional active earth pressure coefficient. They showed that as the aspect ratio decreased, the earth pressure coefficient also decreased, most likely due to the restricted space in which potential slip surfaces could form. Lawson and Yee (2005) used an approach similar to Leshchinsky and Hu to develop design charts for the earth pressure coefficients. They considered planar and bilinear slip surfaces, including composite slip surfaces that passed through the reinforced soil as well as along the interface between the

reinforced soil and the stable face behind the wall. They showed that the forces were less than those for active earth pressures and decreased as the aspect ratio decreased.

Although several researchers have examined the effect of aspect ratio on earth pressures through centrifuge model testing and limit equilibrium and finite difference analyses, the presented study is the first to explore the earth pressure in narrow walls by using the finite element analysis. This study focuses on the at-rest condition and is considered only applicable to the case of a rigid wall or the case of a reinforced wall with inextensible reinforcement.

JANSSENS'S ARCHING THEORY

In 1895 Janssen performed model tests to determine the pressure exerted by corn in a silo. His results showed that the pressure on the bottom of the silo was less than the weight of the corn within the silo. Janssen hypothesized the pressure was transmitted to the side walls and developed an equation to predict the pressure on the sidewall. Janssen's idea can be applied to any granular material, for example, sand in geotechnical engineering. As soil is placed in layers it settles due to its self weight and the load applied by additional soil layers above. Simultaneously, the wall will provide a vertical shear load due to friction that resists the settlement of soil. The vertical shear load reduces the soil overburden pressure and, consequently, reduces the lateral earth pressure. This phenomenon has become known as the arching effect.

Determining the lateral earth pressures in soil resulting from the arching effect was explored by Spangler and Handy in their book entitled *Soil Engineering*. For many engineering purposes it is convenient to work with the non-dimensional lateral earth

pressure coefficient. The coefficient of lateral earth pressure within the backfill for the constrained case is defined as k'. The lateral earth pressure coefficient is given by equation 1 below from Spangler and Handy. Equation 1, referred to as the arching equation henceforth, is based on Janssen's arching theory, but was not proposed in this exact form by Janssen.

$$k' = \frac{1}{2\tan(\delta)} * \left(\frac{b}{z}\right) * \left[1 - \exp\left(-2K\left(\frac{z}{b}\right)\tan(\delta)\right)\right]$$ (1)

where b is the width of the constrained space, z is the depth of the point of interest below the top of the wall, δ is the interface friction angle between the soil and wall, and K is the lateral earth pressure coefficient assuming unlimited space. For the case of an unyielding wall, K was defined by Jaky's empirical formula: $1-\sin(\phi')$ where ϕ' is the angle of internal friction. The lateral earth pressure coefficient depends on the angle of internal friction.

Because Janssens's arching theory was developed to predict lateral earth pressures for boundary conditions similar to those in narrow retaining walls, the theoretical earth pressures are useful when comparing the results of laboratory tests and finite element method simulations. In fact, arching theory is used as one basis for verification of the finite element method.

VERIFICATION OF FINITE ELEMENT METHOD

Establishing confidence in the finite element method to predict lateral earth pressures for unyielding narrow retaining walls was essential to further study. To verify the finite element method, results from finite element simulations were compared to the arching equation and experimental test data.

The Arching Equation

As mentioned in the background section, both Frydman and Take conducted experiments on model retaining walls with narrow backfill widths. The geometries and soil properties from these tests were input into the arching equation (Equation 1) to calculate the lateral earth pressure coefficients. Specific information regarding the model retaining walls can be found in the following sections on the experimental test data and finite element simulations.

Experimental Test Data

Two sets of centrifuge test data were collected for the purpose of verifying the finite element method. The first set of data was from Frydman's centrifuge test (Frydman et al, 1987). Frydman conducted a series of centrifuge tests to investigate the earth pressures on retaining walls near rock faces. The models were built in an aluminum box with inside dimensions 210 mm high x 100 mm wide x 327 mm long. Each model included an aluminum plate (195 mm high x 100 mm wide x 20 mm thick) connected to the base of the box. The rock face was modeled by a wooden block coated with the backfill material, so that the friction between the rock face and the backfill was essentially equal to the angle of internal friction of the backfill. The granular fill between the wall and the rock face was modeled using Haifa Bay uniform fine sand. Particle size was in the range of 0.10-0.30 mm, density between 14.0 - 16.4 kN/m^3 and the sand was placed at a relative density of 70%. Direct shear tests performed on the sand at this relative density gave values of the angle of internal friction (ϕ') equal to 36°. Direct shear tests between the sand and aluminum yielded values of the angles of interface friction (δ) between 20° - 25°.

Load cells (Kyowa, LM-A series) were inset flush with the wall face near the top and bottom of the wall. The model was spun up to 43.7g. The stress levels developed in these models would be similar to those next to full scale walls having a height of about 8.5 m.

The second set of data was from Take's centrifuge test (Take et al, 2001). Take conducted a series of centrifuge tests to investigate the earth pressures on unyielding retaining walls with narrow backfill widths. All model walls were 140 mm high but had various widths corresponding to wall aspect ratios ranging from 0.10 to 0.70. The model backfill material was classified as poorly graded sand with little or no fines. The backfill material had mean particle size equal to 0.4 mm, minimum and maximum dry densities equal to 13.4 and 16.2 kN/m^3, respectively, and relative density equal to 79%. A series of direct shear tests was performed to obtain the angle of internal friction ($\phi'=36^o$), and the interface friction angles with an aluminum wall face ($\delta=23^o$~25°). Six boundary pressure cells were housed and distributed evenly over the height of the model fascia retaining wall. All centrifuge retaining wall experiments were performed at an acceleration of 35.7g which simulates a 5 m high wall at full scale.

Finite Element Modeling

Before performing the finite element analyses, the soil constitutive model, mesh and boundary conditions needed to be chosen. Several options were available when choosing the soil constitutive model. The chosen model should have enough sensitivity to capture the behavior of the soil and soil-wall interaction and the parameters for the model must be obtainable given the information from the literature. The Mohr-Coulomb model was chosen because it fulfilled both requirements. Less complex models did not capture the

soil-wall interaction satisfactorily and more complex models required more parameters than the literature could supply.

A mesh consisting of 15-node triangular elements was generated to represent the backfill because it could determine stresses in the soil more accurately than the alternative choice (6-node triangular elements). In addition to the triangular elements, interface elements were introduce adjacent to the wall face to better capture the soil-wall interaction. The strength of the interface is controlled by the interface reduction factor, R_{inter}. The interface reduction factor is defined as:

$$R_{inter} = \frac{\tan(\delta)}{\tan(\phi')} \qquad (2)$$

where δ is the interface friction angle. The interface reduction factor cannot be greater than unity.

As in the experimental tests, the backfill was constrained by an unyielding wall. To create this condition in the finite element analyses, the boundaries were "fixed". A "fixed" boundary means the nodes along the boundaries were not able to move. Only three boundaries, two side walls and the foundation, were required because the finite element simulations were conducted under plane-strain conditions. An example geometry is shown in Figure 2. Soil properties for the Mohr-Coulomb model are listed in Table1. The geometries and soil properties from Frydman's and Take's centrifuge models were input into the finite element analyses to calculate the lateral earth pressures.
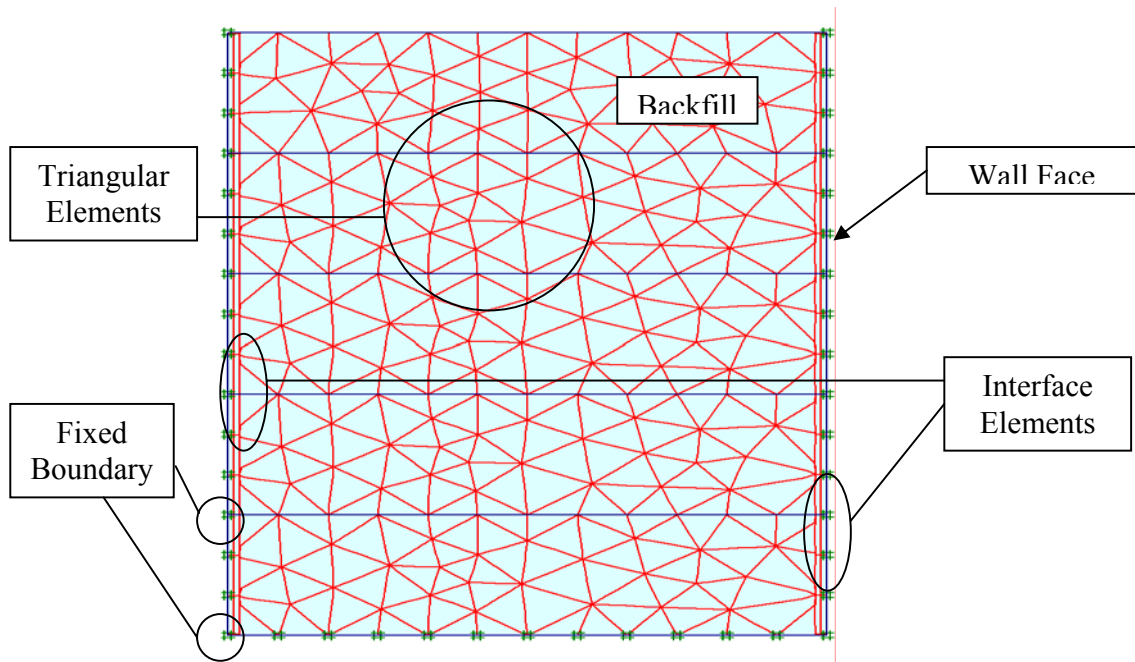
Figure 2 – Example finite element mesh and boundary conditions

Table 1 – Mohr-Coulomb parameters from experimental tests

Symbols	Values		Unit
	Frydman's Test	Take's Test	
Unit weight, γ	16.4	16.2	kN/m^3
Frictional angle, ϕ'	36	36	deg.
Cohesion, C	1	1	kN/m^2
Young's modulus, E	30,000	30,000	kN/m^2
Poisson's ratio, ν	0.3	0.3	--
Interface strength, R_{inter}	0.67	0.67	--

[a] Cohesion was set a small value for numerical purpose

[b] $R_{inter} = \tan\delta/\tan\phi'$

Comparion of Calculated and Measured Earth Pressures

Figure 3 shows the lateral earth pressures from tests by Frydman and Keissar. The results are presented as normalized values. The depth is presented as the non-

dimensional quantity z/L where z is the depth from the top of wall and L is the wall width. Similarly, the lateral earth pressure along the wall is represented by the non-dimensional lateral earth pressure coefficient k_w'. Because of apparent arching effects, the earth pressure coefficients start at the theoretical at-rest value near the top of the wall and decrease with depth below the top of the wall. Except for the divergence at z/L< 0.5, the results of measurements, the arching equation and the finite element simulation agree very well.
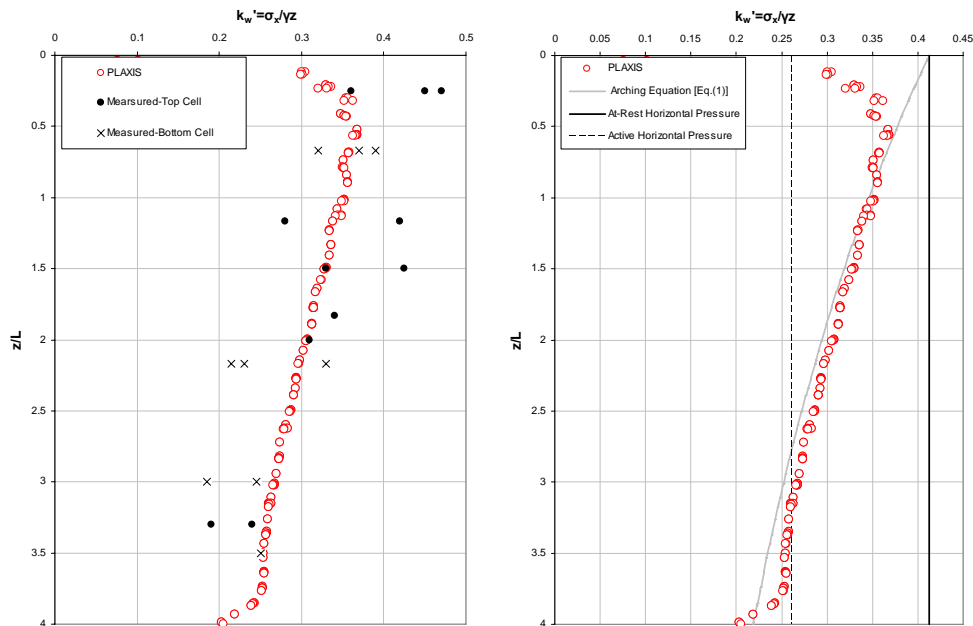
Figure 3 - a (Left): Prediction of earth pressure reduction due to arching effect and compared with Frydman centrifuge test data; b (Right): Prediction of earth pressure reduction due to arching effect and compared with the arching equation
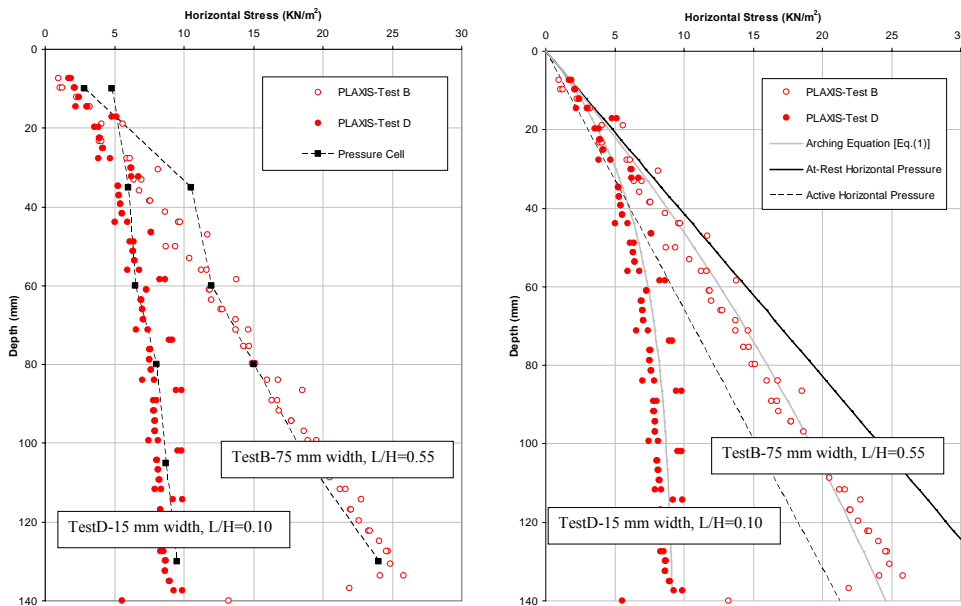
Figure 4 - a (Left): Prediction of earth pressure reduction due to arching effect and compared with Take centrifuge test data; b (Right): Prediction of earth pressure reduction due to arching effect and compared with the arching equation

Figure 4 shows the results from Take's tests, the arching equation and the finite element simulation for two wall aspect ratios. Again, due to arching effects, the earth pressure started at theoretical at-rest values and decreased with depth below the top of the wall; also, the arching effect becomes more prominent as the width of the wall becomes less. In conclusion, the results of measurement, the arching equation and finite element simulation agree very well.

Based on the above comparisons, the finite element method can accurately capture both the arching effect and the reduction of the earth pressure with depth below the top of the wall as the aspect ratio decreases.

EFFECT OF WALL ASPECT RATIO ON LATERAL EARTH PRESSURE FOR UNYIELDING WALLS

Based on the verification of the finite element method, the effect of varying wall aspect ratios on the earth pressures was investigated. Both the earth pressures along a vertical plane adjacent to the face of the wall and along a vertical plane midway between the face of the wall and the rear of the backfill in the at-rest condition were examined. Figures 5 and 6 below show the earth pressure profiles along the wall face and the center of the wall with various wall aspect ratios, respectively. The earth pressures decrease with depth below the surface and with decreasing aspect ratio in both figures. The active (K_a/K_a) and at-rest (K_o/K_a) earth pressure coefficients are also plotted for reference.
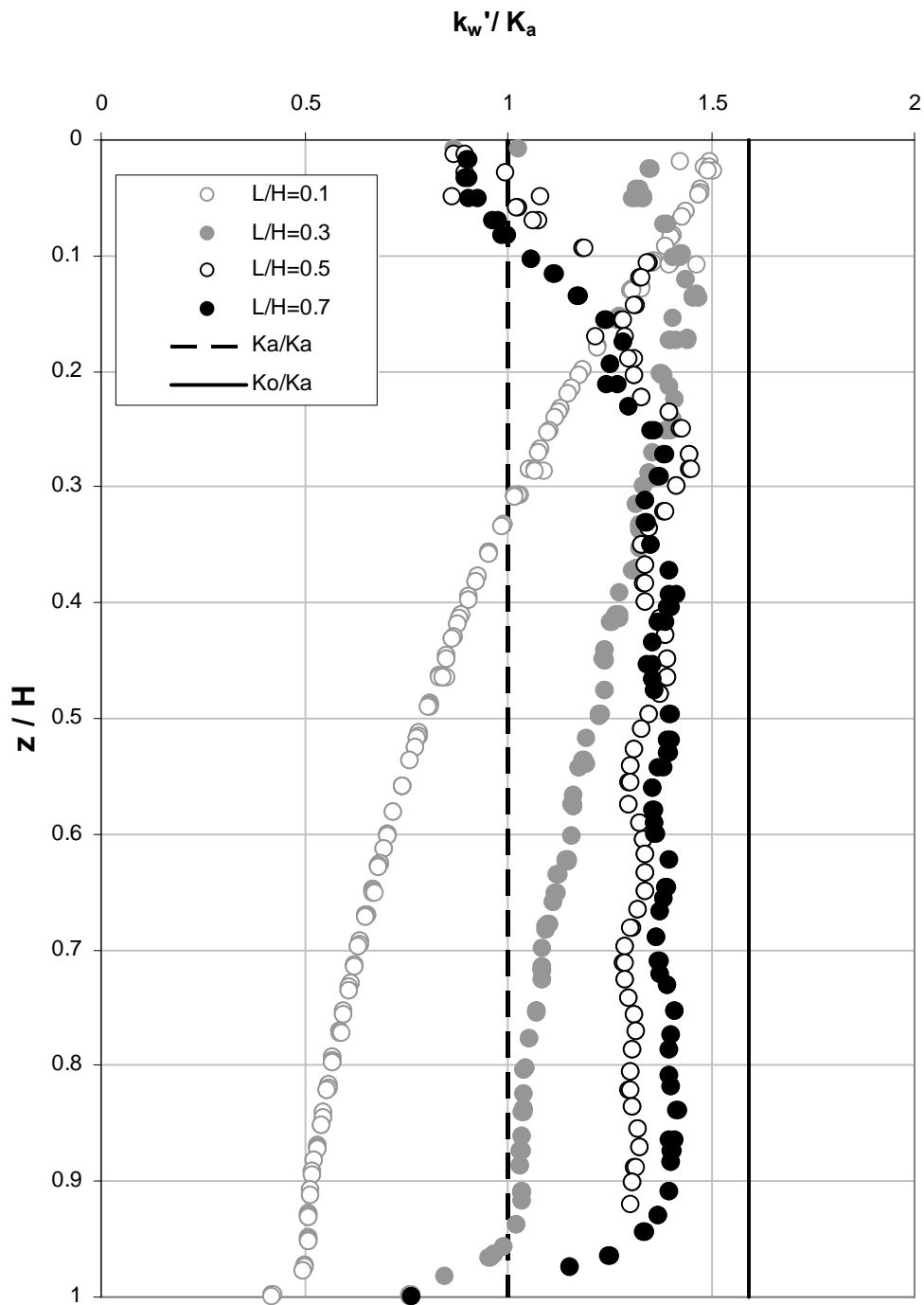
Figure 5 - Variation of normalized earth pressure coefficient profiles along the face of the wall with the wall aspect ratios
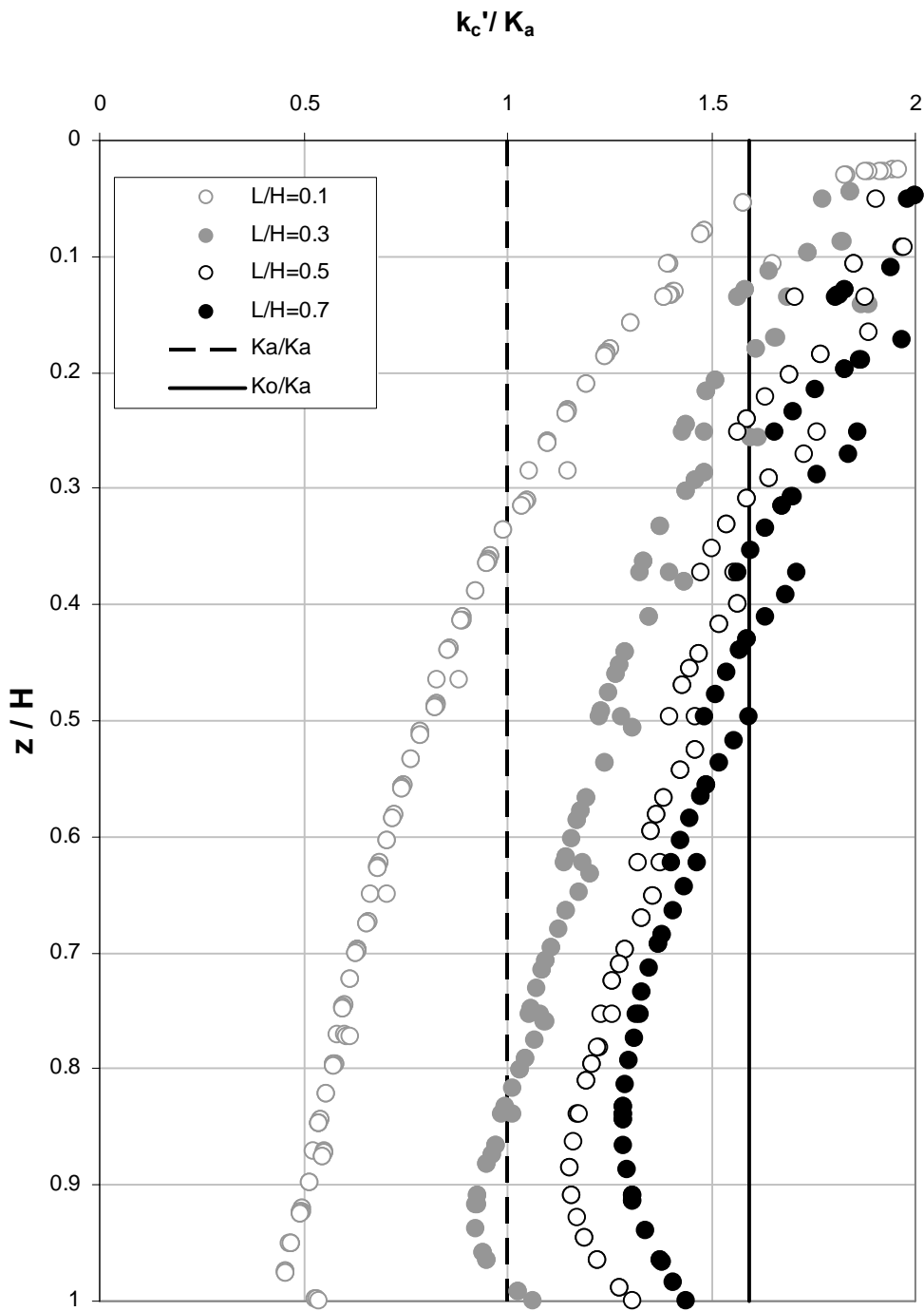
k_c'/ K_a

Figure 6 - Variation of normalized earth pressure coefficient profiles in the center of the
wall with the wall aspect ratios

Comparing the distribution of lateral earth pressure coefficients with depth works well for individual tests like those shown in Figures 3 and 4, however, to compare many tests in this manner would create confusing plots that were difficult to understand. Choosing a maximum or minimum value does not necessarily provide a good indication of the distribution as a whole, and taking the average of the maximum and minimum is misleading if the distribution is non-linear. Thus, the following procedure was used to develop an appropriate indicator of the stress distribution.

By integrating the stress along a vertical plane adjacent to the wall, the equivalent force is obtained. The equivalent force can then be converted to an equivalent lateral earth pressure (K'), using equation 3 below.

$$K' = \frac{F_{eq}}{\frac{1}{2}\gamma H^2} \tag{3}$$

where F_{eq} is the equivalent force acting normal to the wall.

Determining K' was simple for the finite element generated stress distribution because the equivalent force, F_{eq}, is provided in the output. Finding K' was more difficult when using the arching equation. The Trapezoidal Rule was applied to approximate the value of the integral and find the equivalent force. Equation 4 describes the Trapezoidal Rule for any function between two points, a and b.

$$F_{eq} = \int_{a}^{b} f(x)dx = \frac{h}{2}\big(f(a) + f(b)\big) + h * \sum_{i=1}^{n-1} f(a + ih) \tag{4}$$

where the interval from a to b is broken into n equal strips of thickness h. Using an equivalent lateral earth pressure coefficient will allow data from the finite element

15

method, the arching equation and experimental results to be compared for multiple tests in one plot.

To isolate the effect of wall widths on earth pressures, a plot of the equivalent lateral earth pressure (K') vs. wall aspect ratio is shown in Figure 7. The equivalent lateral earth pressure was defined using equations 3 and 4 above. Figure 7 shows the equivalent lateral earth pressures along a vertical plane adjacent to the face of the wall (k'_w), along a vertical plane midway between the face of the wall and rear of the backfill (k'_c) and predicted by the arching equation all agree well with the centrifuge data. The equivalent lateral earth pressures decreased from the at-rest pressure by as much as 60 percent when the aspect ratio decreased to 0.10. Even when the wall aspect ratio was equal to 0.70, which the state-of-practice suggests as a minimum value, the equivalent lateral earth pressure in the center of the wall is around 10% less than the theoretical at-rest pressure. The difference is most likely due to some arching effects. The computed values of K' using the arching equation were slightly less than the calculated lateral earth pressure coefficients using the finite element method.

Although Figure 7 is based on only one soil frictional angle, $\phi'=36°$, Leshchinsky and Hu suggest that normalizing the lateral earth pressure coefficient in walls with narrow backfills by the Rankine active earth pressure coefficient significantly reduces scatter over a range of friction angles. Leshchinsky and Hu found the ratios did not vary more than 3 percent between friction angles of 25° and 45°. However, engineers should use Figure 7 carefully because the backfill of the narrow MSE wall is limited to gravel or sand materials. Figure 7 is not appropriate when using locally, naturally cohesive materials as backfill because the arching effect in cohesive materials has been questioned.
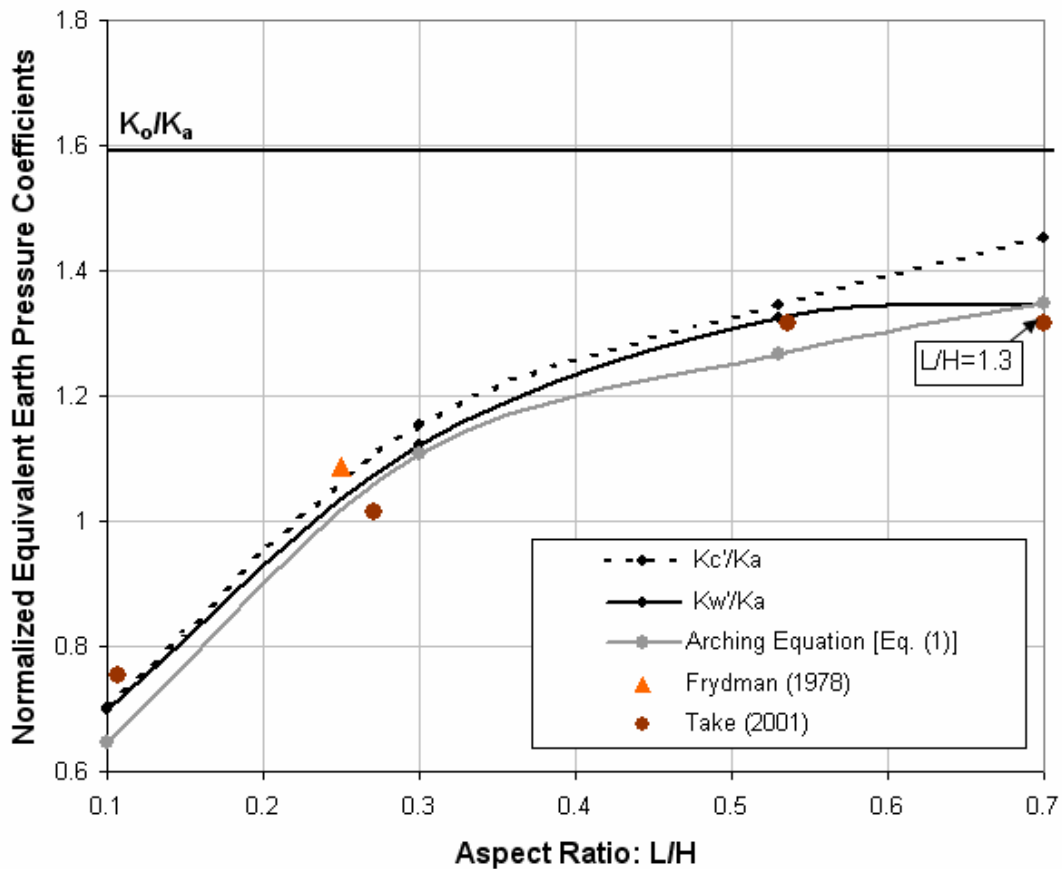
16

Figure 7 – Normalized equivalent earth pressure coefficient along the wall and in the
center of the backfill with wall aspect ratios

COMPARISON OF PREDICTED LATERAL EARTH PRESSURE TO
FHWA DESIGN GUIDELINES

For comparison, the earth pressures calculated from the finite element analyses for different wall aspect ratios were plotted with the design earth pressures according to the FHWA MSE wall design guidelines in Figure 8. The earth pressure from the finite element analyses are based on the earth pressures profile along a vertical plane midway between the face of the wall and rear of the backfill, which is also the maximum earth pressures profile in the case of the at-rest condition. The earth pressure profile from the

finite element analyses for a wall aspect ratio equal to 0.70 corresponds well with the guidelines for metal bars, mats and welded wire grids, i.e. very stiff, inextensible reinforcement. Comparisons for more flexible reinforcement and using yielding walls with the finite element method are currently underway. The earth pressures found in Figure 8 also indicate that as the wall aspect ratio decreases, the earth pressure coefficients also decrease.
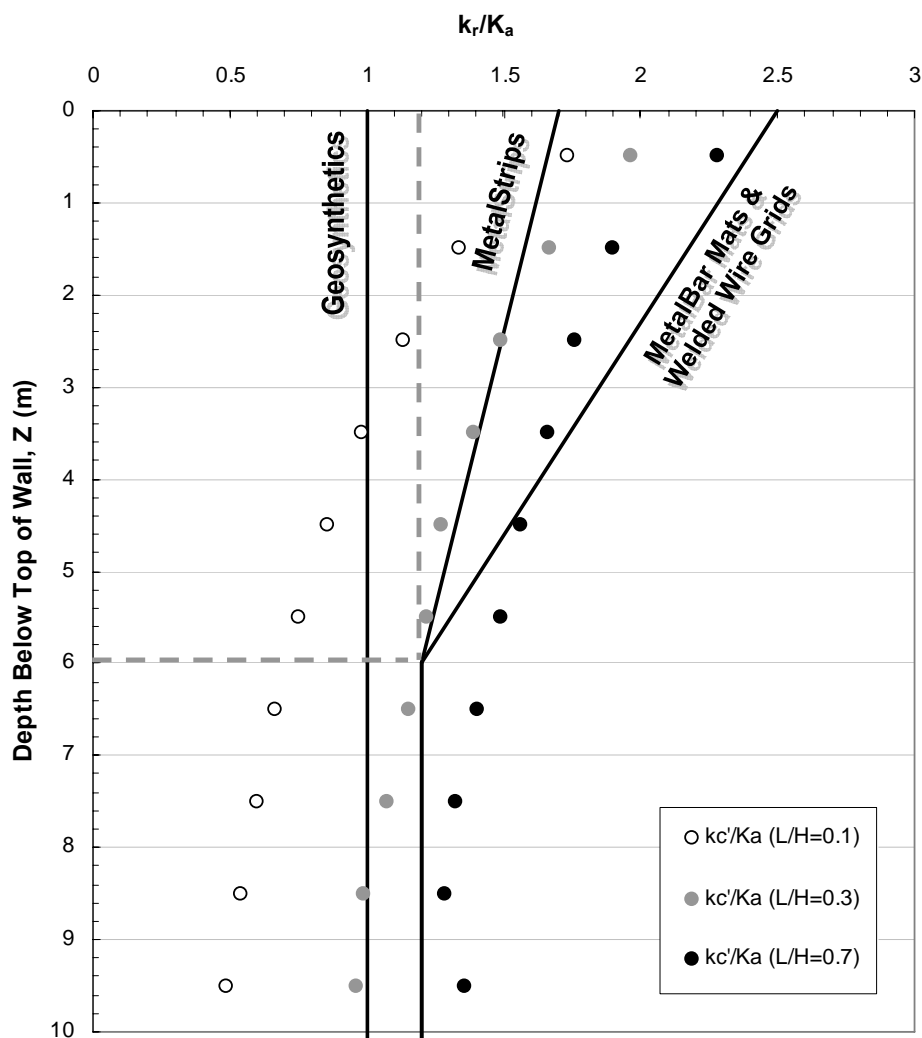

Figure 8 - Normalized earth pressure coefficient profiles in the center of the wall with the FHWA MSE wall design chart

CONCLUSION

Demands for increasing capacity of existing highways has resulted in the need for adding traffic lanes. This often involves construction of new retaining walls in limited space and in front of existing stable walls or slopes. Walls often dictate widths less than the normal width of 70 percent of the wall height. Consequently the earth pressures are likely to be different from those for walls of more conventional larger widths.

A series of finite element analyses was performed to investigate the earth pressures behind walls with less than the normal width. These analyses were performed for non-yielding walls such as those with very stiff, inextensible reinforcement. The earth pressures calculated by the finite element method were then compared to pressures calculated from the arching equation as well as measured values from centrifuge tests on narrow walls with low aspect ratios. Favorable agreement was found between the calculated pressures from finite element analyses and those from the arching equation and experimental measurements. All show that the earth pressures generally become smaller as the wall aspect ratio decreases.

The earth pressures calculated by the finite element method were also compared with those in the FHWA criteria for MSE walls. The results for walls with the normal aspect ratio (L/H) of 0.70 showed good agreement with the recommended values for walls with stiff, inextensible reinforcement. However, significantly lower pressures are indicated from the finite element analyses for walls with lower aspect ratios.

ACKNOWLEDGEMENTS

Notation

The following symbols are used in this paper

a: lower bound of function approximated by Trapezoidal Rule;

b: upper bound of function approximated by Trapezoidal Rule, also width of constrained

space;

C: cohesion;

E: Young's modulus;

h: thickness of element used in Trapezoidal Rule;

H: wall height;

i: index used to keep track of elements in Trapezoidal Rule;

k': calculated earth pressure coefficient for the constrained case;

    k_c': calculated earth pressure coefficient along vertical plane midway between the

        face of the wall and rear of the backfill;

    k_w': calculated earth pressure coefficient along a vertical plane adjacent to the face of

        the wall;

K: earth pressure coefficient for the case of unlimited space;

  K_o: Jaky's at-rest earth pressure coefficient, $Ko=1-\sin\phi'$;

  K_a: Rankine active earth pressure coefficient, $Ka=\tan^2(45^o-\phi'/2)$;

K': equivalent lateral earth pressure coefficient for the constrained case;

    K_c': calculated equivalent earth pressure along vertical plane midway between the

        face of the wall and rear of the backfill;

    K_w': calculated equivalent earth pressure along a vertical plane adjacent to the face of

        the wall;

L: wall width;

n: number of elements of equal thickness, h, used in Trapezoidal Rule;

$\mathbf{R_{inter}}$**:** interface reduction factor;

z: depth below the top of the wall;

$\boldsymbol{\delta}$**:** interface frictional angle;

$\boldsymbol{\phi'}$**:** effective frictional angle;

$\boldsymbol{\gamma}$**:** unit weight;

$\boldsymbol{\nu}$**:** Poisson's ratio**;**

References

Elias, V., Christopher, B.R., and Berg, R.R., (2001), "Mechanically Stabilized Earth Walls and Reinforced Soil Slopes Design and Construction Guidelines," *Report No. FHWA-NHI-00-043*, National Highway Institute, Federal Highway Administration, Washington, D.C., March.

Frydman, S. and Keissar, I., (1987), "Earth pressure on retaining walls near rock faces," *Journal of Geotechnical Engineering,* ASCE*,* Vol. 113, No. 6, June, pp. 586-599.

Lawson, C.R., and Yee, T.W., (2005), "Reinforced soil retaining walls with constrained reinforced fill zones," *Proceedings*, *Geo-Frontiers 2005*, ASCE Geo-Institute Conference, pp. 2721-2734.

Leshchinsky, D., Hu, Y. and Han, J., (2004), " Limited reinforced space in segmental retaining walls," *Geotextiles and Geomembranes*, Vol. 22, No. 6, pp. 543-553.

Plaxis (2005). *Plaxis Finite Element Code for Soil and Rock Analyses*, Version 8.2, P.O. Box 572, 2600 AN Delft, The Netherlands (Distributed in the United States by GeoComp Corporation, Boxborough, MA).

Spangler, M. and Handy, R. *Soil Engineering*. New York: Harper and Row, 1982

Sperl, M. "Experiments on corn pressure in silo cells – translation and comment of Janssen's paper from 1895," *Granular Matter*, Vol. 8, pp.59-65, December 2006.

Take, W.A. and Valsangkar (2001), "Earth pressures on unyielding retaining walls of narrow backfill width," *Can. Geotech. Journal,* Vol.38, pp.1220-1230.

Woodruff, R. (2003), "Centrifuge modeling of MSE-shoring composite walls," Thesis submitted to the faculty of the Graduate School of the University of Colorado in partial fulfillment of the requirements for the Master of Science degree, Department of Civil Engineering, Boulder.